



## A novel approach for enhancing the signal-to-noise ratio and detecting automatically event-related potentials (ERPs) in single trials

L. Hu <sup>a,b,c</sup>, A. Mouraux <sup>d</sup>, Y. Hu <sup>c</sup>, G.D. Iannetti <sup>a,b,\*</sup>

<sup>a</sup> Department of Neuroscience, Physiology and Pharmacology, University College London, UK

<sup>b</sup> Department of Physiology, Anatomy and Genetics, University of Oxford, UK

<sup>c</sup> Department of Orthopaedics and Traumatology, The University of Hong Kong, Hong Kong, China

<sup>d</sup> Unité READ, Université catholique de Louvain, Brussels, Belgium

### ARTICLE INFO

#### Article history:

Received 15 September 2009

Revised 25 November 2009

Accepted 1 December 2009

Available online 11 December 2009

#### Keywords:

Laser-evoked potentials (LEPs)

N1 wave

Single-trial analysis

Independent component analysis (ICA)

Wavelet filtering

Multiple linear regression

Event-related potentials (ERPs)

### ABSTRACT

Brief radiant laser pulses can be used to activate cutaneous A $\delta$  and C nociceptors selectively and elicit a number of transient brain responses in the ongoing EEG (N1, N2 and P2 waves of laser-evoked brain potentials, LEPs). Despite its physiological and clinical relevance, the early-latency N1 wave of LEPs is often difficult to measure reliably, because of its small signal-to-noise ratio (SNR), thus producing unavoidable biases in the interpretation of the results. Here, we aimed to develop a method to enhance the SNR of the N1 wave and measure its peak latency and amplitude in both average and single-trial waveforms. We obtained four main findings. First, we suggest that the N1 wave can be better detected using a central-frontal montage (Cz-Fz), as compared to the recommended temporal-frontal montage (Tc-Fz). Second, we show that the N1 wave is optimally detected when the neural activities underlying the N2 wave, which interfere with the scalp expression of the N1 wave, are preliminary isolated and removed using independent component analysis (ICA). Third, we show that after these N2-related activities are removed, the SNR of the N1 wave can be further enhanced using a novel approach based on wavelet filtering. Fourth, we provide quantitative evidence that a multiple linear regression approach can be applied to these filtered waveforms to obtain an automatic, reliable and unbiased estimate of the peak latency and amplitude of the N1 wave, both in average and single-trial waveforms.

© 2009 Elsevier Inc. All rights reserved.

### Introduction

The magnitude of event-related EEG responses is often several factors smaller than the magnitude of the background ongoing EEG. Therefore, the identification and characterization of the EEG responses elicited by sensory events (event-related potentials, ERPs) rely on signal processing methods for enhancing their SNR. The most widely used approach is the across-trial averaging in the time domain (Dawson, 1951, 1954). The obtained waveform expresses the average scalp potential as a function of time relative to the onset of the sensory event. The basic assumption underlying this procedure is that ERPs are stationary (i.e., their latency and morphology are invariant across trials) and will therefore be unaffected by the averaging procedure, while the ongoing electrical brain activity behaves as noise unrelated to the event, and will therefore be largely cancelled out by the averaging procedure, thus enhancing the SNR of ERPs (Mouraux and Iannetti, 2008).

The cost of this across-trial averaging procedure is that all the information concerning across-trial variability of ERP latency and

amplitude is lost. However, this variability may reflect important factors such as differences in stimulus parameters (duration, intensity, and location) (Iannetti et al., 2005b, 2006; Mayhew et al., 2006), and, most importantly, fluctuations in vigilance, expectation, attentional focus, or task strategy (Haig et al., 1995). Hence, the ability to obtain a reliable single-trial estimate of ERP latency and amplitude would allow exploring the single-trial dynamics between these ERP measures, behavioural variables (e.g. intensity of perception, reaction time) (Iannetti et al., 2005b) and also measurements of brain activity obtained using different neuroimaging modalities (e.g. fMRI) (Mayhew et al., 2010). Therefore, methods that explore ERP dynamics at the level of single-trials can provide new insights into the functional significance of the different processes underlying these brain responses (for a review see Mouraux and Iannetti, 2008).

Brief radiant heat pulses, generated by infrared laser stimulators, excite selectively A $\delta$ - and C-fibre free nerve endings located in the superficial layers of the skin (Bromm and Treede, 1984). Such stimuli elicit a number of brain responses that can be detected in the human EEG both in the time domain (laser-evoked potentials, LEPs; Carmon et al., 1976) and in the time-frequency domain (Mouraux et al., 2003). LEPs are related to the activation of type-II A-mechano-heat nociceptors (Treede et al., 1998) and spinothalamic neurons located in the anterolateral quadrant of the spinal cord (Treede et al., 2003).

\* Corresponding author. Department of Neuroscience, Physiology and Pharmacology, Medical Sciences Building, Gower Street, London, WC1E 6BT, UK. Fax: +44 20 7679 7928.  
E-mail address: g.iannetti@ucl.ac.uk (G.D. Iannetti).

They comprise a number of waves that are time locked to the onset of the stimulus. The largest wave is a negative-positive complex maximal at the scalp vertex (N2–P2, peaking at 200–350 ms when stimulating the hand dorsum) (Bromm and Treede, 1984). This complex is preceded by a smaller negative wave (N1) that overlaps in time and space with the larger subsequent N2 wave, and is described as having a distribution maximal over the temporal region contralateral to the stimulated side. In order to isolate the N1 wave from the N2 wave, the N1 is usually detected at the contralateral temporal electrode (Tc) referred to a frontal midline electrode (Fz or Fpz) (Fig. 1, top left panel), an EEG montage that is also recommended for recording LEPs in clinical settings (Cruccu et al., 2008; Kunde and Treede, 1993; Treede et al., 2003). Several studies have shown that the N1, N2 and P2 waves reflect a combination of cortical activities originating from primary and secondary somatosensory cortices, the

insula, and the anterior cingulate cortex (Cruccu et al., 2008; Garcia-Larrea et al., 2003).

While the N2 and P2 waves are characterized by a high SNR (with a peak-to-peak amplitude of several tens of microvolts when averaging 20–30 trials) and can be easily detected in single trials (Carmon et al., 1980; Iannetti et al., 2005b), the N1 wave has a smaller SNR and is thus more difficult to detect. This difficulty is not only due to the fact that the N1 wave is generated by neural activities of smaller magnitude than those underlying the N2 and P2 waves (Cruccu et al., 2008; Treede et al., 2003). It is also due to the fact that the N1 and N2 waves (Kunde and Treede, 1993) overlap in time and space with opposite polarities, and to the fact that temporal electrodes are often contaminated by artifacts related to the activity of the *temporalis* muscle. For all these reasons, the vast majority of physiological (Iannetti et al., 2003) and clinical (Treede et al., 2003) LEP studies

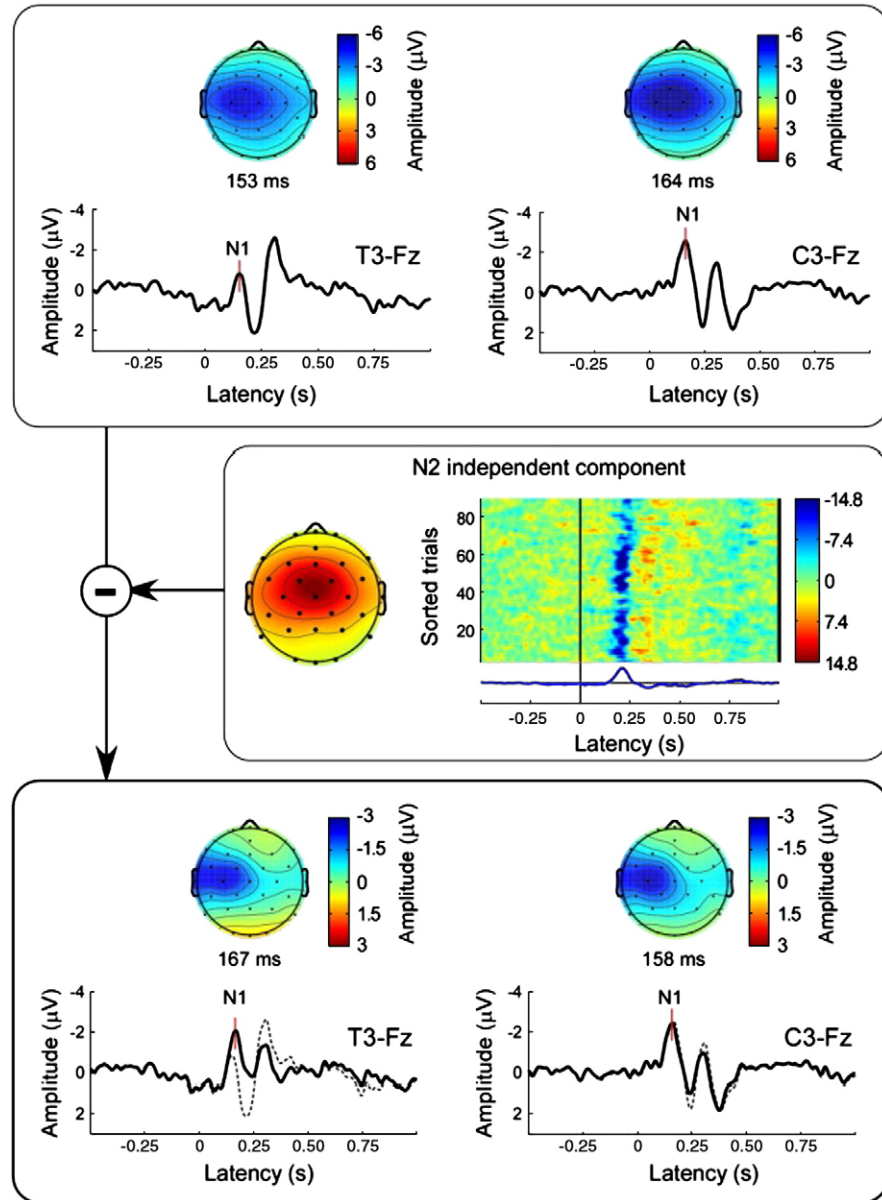


**Fig. 1.** Effect of montage and ICA removal on the time course and scalp topography of the N1 response. Top panel: group average time courses of N1 response in the “T3-Fz” and “C3-Fz” conditions are shown as black waveforms (solid line). Scalp topographies are displayed at the peak latency of the N1 wave (latencies marked as red vertical lines). Middle panel: representative N2-related activity was identified using ICA, and subtracted from the data. The scalp topography of an IC capturing the N2-related activity is shown on the left. Note that, in this IC, electrodes C3 and Fz display a similar weight, heavier than that at electrode T3. This explains why the N2-related IC removal affects the “Tc-Fz” condition more than the “Cc-Fz” condition (shown in the bottom panel). Bottom panel: group average time courses of N1 responses after the removal of N2 ICs. Waveforms obtained after subtraction are shown in black (solid lines), whereas waveforms before subtraction are shown in grey (dashed lines). Scalp topographies are displayed at the peak latency of the N1 wave (latencies marked as red vertical lines).

conducted in the past 30 years have relied uniquely on measures of the N2 and P2 waves to investigate the nociceptive system. In recent years, a growing number of studies have started to explore experimental modulations of the latency and amplitude of the N1 wave, and to characterize its functional significance (Ellrich et al., 2007; Iannetti et al., 2008; Lee et al., 2009; Legrain et al., 2002; Mouraux and Iannetti, 2009; Schmahl et al., 2004). Indeed, there is experimental evidence indicating that the N1 wave represents an early stage of sensory processing more directly related to the ascending nociceptive input (Lee et al., 2009), while the later N2 and P2 waves appear to reflect neural activities largely unspecific for the sensory modality of the eliciting stimulus (Mouraux and Iannetti, 2009). For all these reasons, a more systematical examination of N1 has been recommended to enhance the sensitivity of LEPs in clinical applications (Cruccu et al., 2008; Treede et al., 2003).

Hence, a technique to assess reliably the magnitude of the N1 wave has been long awaited by the scientific community, and its availability would represent a significant improvement for a more complete utilization of LEPs to explore the nociceptive system. Here we describe a novel method that combines independent component analysis (ICA) with wavelet filtering and multiple linear regression to obtain automatic and unbiased measures of latency and amplitude of ERPs, both in averaged and single-trial responses. When applied to LEPs, we show that this method provides a reliable estimate of the latency and amplitude of the N1 peak at single-trial level.

## Methods

### Subjects

EEG data were collected from eleven healthy volunteers (eight females and three males) aged from 23 to 42 years ( $30 \pm 5$ , mean  $\pm$  SD). All participants gave written informed consent, and the local ethics committee approved the procedures.

### Nociceptive stimulation and experimental paradigm

Noxious radiant-heat stimuli were generated by an infrared neodymium yttrium aluminium perovskite (Nd:YAP) laser with a wavelength of 1.34  $\mu\text{m}$  (Electronical Engineering, Italy). These laser pulses activate directly nociceptive terminals in the most superficial skin layers (Baumgartner et al., 2005; Iannetti et al., 2006). Laser pulses were directed to the dorsum of the right hand and a He-Ne laser pointed to the area to be stimulated. The laser pulse was transmitted via an optic fibre and focused by lenses to a spot diameter of approximately 8 mm (50  $\text{mm}^2$ ) at the target site. The duration of the laser pulses was 4 ms and its energy 3.5 J. With these parameters laser pulses elicit a clear pinprick sensation, related to the activation of  $\text{A}\delta$  skin nociceptors (Iannetti et al., 2006). After each stimulus, the laser beam target was shifted by approximately 20 mm in a random direction, to avoid nociceptor fatigue and sensitization. The laser beam was controlled by a computer that used two servo-motors (HS-422; Hitec RCD, USA; angular speed, 60°/160 ms) to orient it along two perpendicular axes (Lee et al., 2009).

### EEG recording

EEG data were collected in a single recording session, comprising three blocks of stimulation. In each block, 30 trials were presented with an inter-trial interval (ITI) ranging between 15 and 18 s. Participants were seated in a comfortable chair and wore protective goggles. They were asked to focus their attention on the stimuli, relax their muscles and keep their eyes open and gaze slightly downward. Acoustic isolation was ensured using earplugs and headphones. Both the laser beam and the controlling motors were completely screened from the view of the participants. The EEG was

recorded using 30 Ag-AgCl electrodes placed on the scalp according to the International 10-20 system, using the nose as extracephalic reference. To monitor ocular movements and eye blinks, electro-oculographic (EOG) signals were simultaneously recorded from two surface electrodes, one placed over the lower eyelid, the other placed 1 cm lateral to the outer corner of the orbit. The electrocardiogram was recorded using two electrodes placed on the dorsal aspect of the left and right forearms. Signals were amplified and digitized using a sampling rate of 1,024 Hz and a precision of 12 bits, giving a resolution of  $0.195 \mu\text{V digit}^{-1}$  (System Plus; Micromed, Italy).

### EEG data preprocessing

EEG data were imported and processed using EEGLAB (Delorme and Makeig, 2004), an open source toolbox running under the MATLAB environment. Continuous EEG data were band-pass filtered between 1 and 30 Hz. EEG epochs were extracted using a window analysis time of 1500 ms (500 ms pre-stimulus and 1000 ms post-stimulus) and baseline corrected using the pre-stimulus time interval. In order to test the possible bias in the automated single-trial N1 detection method, the same number of trials of resting EEG (3500 ms to 5000 ms post-stimulus) were extracted from the dataset of each subject.

Trials contaminated by eye-blanks and movements were corrected using an ICA algorithm (Delorme and Makeig, 2004; Jung et al., 2001; Makeig et al., 1997). EEG epochs were then visually inspected and trials contaminated by artifacts due to gross movements were removed. In all datasets, individual eye movements, showing a large EOG channel contribution and a frontal scalp distribution, were clearly seen in the removed independent components.

After these pre-processing steps, 987 epochs remained for the automated N1 detection. Similarly, 987 epochs of resting EEG were kept for testing the possible detection bias.

### EEG data analysis: standard averaging for N1 detection

For each subject, average waveforms were computed, time-locked to the onset of the stimulus. Single-subject average waveforms were subsequently averaged to obtain group-level average waveforms. For each waveform, the latency and the baseline-to-peak amplitude of N1 were measured in two conditions: at the temporal electrode contralateral to the stimulated side, referenced to Fz (T3-Fz), i.e. the recommended montage to detect N1 (Treede et al., 2003), and at the central electrode contralateral to the stimulated side, referenced to Fz (C3-Fz). N1 was defined as the negative deflection preceding the N2 wave, which appears, in this montage, as a positive deflection. Unique and obvious negative deflections preceding the N2 wave were classified as a clear N1 response, while the N1 response was defined as absent if the N1 amplitude was positive or if a unique negative deflection preceding the N2 wave could not be identified. Group-level scalp topographies at the latency of the N1 wave were computed by spline interpolation.

For each subject, epoched EEG data were decomposed using ICA (runica routine; Delorme and Makeig, 2004), a technique used successfully by a growing number of investigators to perform blind source separation of scalp EEG (Makeig et al., 1997, 2004). When applied to multi-channel recordings, ICA unmixes the signals recorded on the scalp into a single linear combination of independent components (ICs), each having a maximally independent time course and a fixed scalp distribution. In each subject, we searched for ICs reflecting the N2 activity.

ICs were classified as being “N2-related” when they satisfied the following three criteria: (1) Being stimulus-related, i.e. reflecting neural activity elicited by the laser stimulus. To ascertain this, the time course of the power of each IC ( $\mu\text{V}^2$ ) was expressed as the standard

deviation from the mean (*Z* scores) of the pre-stimulus interval (−500 to 0 ms). In each IC, the *Z* scores were then averaged within the 0 to +500 ms post-stimulus interval. Only if the resulting average *Z* score was larger than 5, the IC was classified as stimulus-related (the same approach used in Mouraux and Iannetti, 2009). (2) Having the latency of the first peak comprised between 175 and 275 ms. (3) Having a scalp topography centrally-distributed and maximal at the vertex (Fig. 1, middle panel).

These ICs were subsequently removed, thus generating a new set of EEG data devoid of the N2-related activity represented in these components.

New average waveforms were computed from this new dataset, using the procedures described previously. Such as for the original EEG data, the baseline-to-peak amplitude of the N1 wave was measured at the temporal electrode contralateral to the stimulated side, rereferenced to Fz (T3-Fz, N2-IC removed), and at the central electrode contralateral to the stimulated side, also rereferenced to Fz (C3-Fz, N2-IC removed). Also for these additional two conditions group-level scalp topographies at the latency of the N1 wave were computed.

The latency and amplitude of the N1 wave obtained in each of these four conditions "T3-Fz", "C3-Fz", "T3-Fz, N2-IC removed" and "C3-Fz, N2-IC removed" were compared using a two-way, repeated measures analysis of variance (ANOVA), using "montage" and "N2-IC removal" as experimental factors. When significant, *post hoc* paired *t* tests were used to perform pairwise comparisons. All statistical analyses were carried out using SPSS 16.0 (SPSS Inc., Chicago, IL).

#### EEG data analysis: single-trial analysis of N1

The method for estimating the latency and amplitude of the N1 wave in single trials, summarized in Fig. 2, consists of two consecutive steps: wavelet filtering and multiple linear regression. This method has been developed into user-friendly software running under the Matlab environment, which can be freely downloaded from <http://iannettilab.webnode.com>.

#### Wavelet filtering

Single-trial N1 waveforms from the "C3-Fz, N2-IC removed" condition were wavelet-filtered to reduce the background noise as well as part of the N2-P2 response, and increase the SNR of the N1 response. Wavelet filtering was performed in the following three steps (detailed below). First, single-trial N1 waveforms were decomposed into a time-frequency representation using a continuous wavelet transform (CWT). Second, specific areas on the time-frequency plane corresponding to the N1 response (group average) were identified and used to generate the wavelet filtering model. Third, time-domain N1 waveforms were reconstructed using an inverse continuous wavelet transform (ICWT).

##### (a) Continuous wavelet transform (CWT)

Unlike the windowed Fourier transform, the continuous wavelet transform (CWT) is able to construct a time-frequency representation of EEG or ERP signals that offers an optimal compromise for time and frequency resolution by adapting the window width as a function of estimated frequency (Iannetti et al., 2008; Mouraux et al., 2003; Mouraux and Iannetti, 2008). The time-frequency representation obtained by CWT provides a relatively low temporal resolution but a

high frequency resolution at low frequencies, and a relatively high temporal resolution but a low-frequency resolution at high frequencies, and is thus well suited to explore transient modulations of the EEG spectrum within a wide frequency spectrum (Iannetti et al., 2008).

The CWT has a linear distribution and is defined as (Tognola et al., 1998):

$$WT(\tau, f) = \int_t x(t) \cdot \sqrt{f/f_0} \cdot \psi^*(f/f_0 \cdot (t - \tau)) dt \quad (1)$$

$$\psi(t) = \frac{1}{\sqrt{\pi f_b}} e^{2\pi i f_0 x} e^{-\frac{t^2}{f_b}} \quad (2)$$

where  $\tau$  and  $f$  are the time and frequency index, respectively, and  $x(t)$  is the original signal in time ( $t$ ) domain;  $\psi(t)$  is the mother wavelet function with central frequency  $f_0$ . The mother wavelet  $\psi(t)$  used in this study is a complex Morlet wavelet (Eq. (2)). Bandwidth parameters  $f_b$  and  $f_0$  were set to 0.05 and 6, respectively, and display a good time-frequency resolution with explored frequencies ranging from 1 to 30 Hz in steps of 0.3 Hz. The squared magnitude of  $WT(\tau, f)$  is called the scalogram or power spectrum.

##### (b) Wavelet filtering model

In order to apply time-frequency filtering to enhance the SNR of the N1 response at the level of single trials, a weighted, binary time-frequency template ( $W_f$ ) was generated, identifying the distribution of EEG changes induced by the laser stimulus contained in the grand-averaged time-frequency matrix. This template was then used to filter out the contribution of non-stimulus-related background activity, as well as the contribution of part of the N2-P2 response, and thereby enhance the SNR of the N1 response.

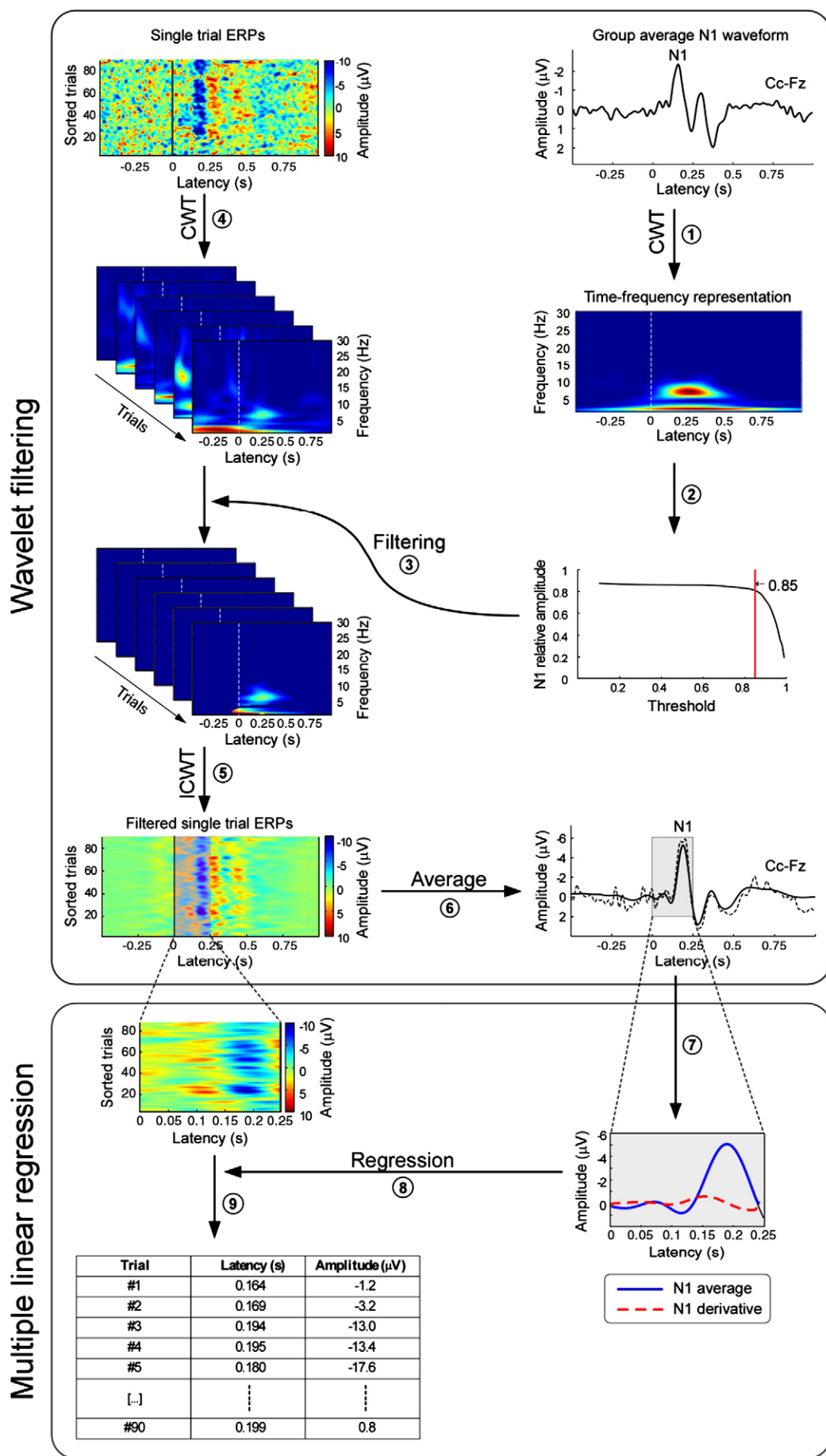
For each estimated frequency, the magnitude of the power spectrum was baseline-corrected by subtracting the average power of the signal enclosed in the time-interval ranging between −250 and 0 ms (Iannetti et al., 2008; Pfurtscheller and Lopes da Silva, 1999). The obtained time-frequency matrix was then thresholded with the objective of keeping wavelet coefficients with high energy and eliminating wavelet coefficients with low energy. The empirical cumulative distribution function (CDF) of normalized power spectrum was calculated by the Kaplan-Meier estimate (Lawless, 2003), and the filtering model was obtained by creating a matrix whose time-frequency pixels were set to 1 when the CDF of the corresponding wavelet coefficient was greater than the threshold, and set to 0 when the CDF of the corresponding wavelet coefficient was smaller than the threshold, defined as  $0.85 \times (\max(CDF) - \min(CDF)) + \min(CDF)$ . As shown in Fig. 2 (step 3), the selected threshold was set just before the inflection point, with the objective of keeping the greater part of the N1 response while removing as much noise as possible.

For each single trial EEG epoch, time-frequency filtering was achieved by Eq. (3).

$$FWT_i(\tau, f) = W_f \cdot WT_i(\tau, f) \quad (3)$$

where  $WT_i$  is the time frequency representation of trial  $i$  obtained by CWT, and  $FWT_i$  is the filtered time frequency representation which is calculated by multiplying  $WT_i$  with the previously computed filtering matrix  $W_f$ .

**Fig. 2.** Flowchart describing the procedure developed to enhance the SNR of the N1 wave of LEPs (top panel), and to measure automatically its peak latency and amplitude in single trials (bottom panel). Top panel: a time-frequency representation is obtained from group average waveform, using a continuous wavelet transform (CWT) (1), and a wavelet filter is generated by thresholding this time-frequency representation (2). This filter is applied (3) to the time-frequency representation obtained from single-trial LEP responses (4). Filtered single-trial LEP responses are then reconstructed in the time-domain using an inverse CWT (ICWT) (5), and finally averaged (6). This procedure generates both single-trial (5) and averaged (6) LEP responses with enhanced SNR. Bottom panel: a multiple linear regression is applied to these single-trial LEPs with enhanced SNR to obtain a fast and unbiased estimate of the peak latency and amplitude of N1 waves. A regressor and its temporal derivative (0 to 0.25 s post-stimulus) are obtained from the across-trial average waveform (7). This basis set is then regressed (8) against the corresponding time window of each single LEP trial, thus yielding (9) a latency and amplitude value for each N1 peak.



(c) Inverse continuous wavelet transform (ICWT)

The time–frequency filtered signal  $y_i(t)$  was reconstructed into the time domain by applying the inverse continuous wavelet transform (ICWT) to the filtered time–frequency distribution  $\text{FWT}_i(\tau, f)$  with the following expression (Tognola et al., 1998).

$$y_i(t) = C_\psi \int \int \text{FWT}_i(\tau, f) \cdot \sqrt{f/f_0} \cdot \psi(f/f_0(t - \tau)) \cdot (f/f_0)^2 d\tau \cdot df \quad (4)$$

where  $C_\psi$  is a coefficient that depends on the Fourier transform of  $\psi(t)$ .

The SNR was estimated by dividing the N1 peak amplitude (absolute value) by the standard deviation of the LEP waveform in the pre-stimulus interval (−500 to 0 ms), an approach proposed by some investigators (e.g. Debener et al., 2007; Spencer, 2005). SNR values before and after wavelet filtering were assessed using non-parametric Wilcoxon test, due to the non-normal distribution of the SNR values.

#### Multiple linear regression

In order to estimate N1 latency and amplitude in an accurate and unbiased fashion, a linear regression method similar to the one we originally described in Mayhew et al. (2006) was applied to the wavelet filtered data, within the 0–250 ms post-stimulus time-interval.

The linear regression model can be written as:

$$\mathbf{Y} = \sum_{i=1}^2 \beta_i \mathbf{X}_i + \epsilon \quad (5)$$

where  $\mathbf{Y}$  is a  $m \times n$  matrix containing  $m$  single-trials EEG epochs and  $n$  samples of each epoch (from 0 ms to the first zero crossing point after the N1 peak).  $\mathbf{X}_i$  are the regressors derived from the average waveform.  $\beta_i$  are coefficients that weight the fit of  $\mathbf{X}_i$  to the data  $\mathbf{Y}$ .  $\epsilon$  is the residual error of the fitted model.

For each subject, a regressor and its temporal derivative were obtained from the across-trial average waveform measured after wavelet filtering. The inclusion of the temporal derivative allows modeling the temporal variability of the response and provides an estimate of single-trial N1 wave latency. This basis set was then regressed against each single EEG epoch. The coefficients  $\beta_i$  of each trial were calculated by multiple linear regression, and the corresponding fit of the N1 response was obtained by multiplying the two regressors (derived from the average waveform, see Eq. 5) by the regression coefficients.

Based on the fitted waveform, latency and amplitude of the N1 response in each single trial was estimated by finding the most negative peak if  $\beta_1 > 0$  (positive fit), or the most positive peak if  $\beta_1 < 0$  (negative fit) within an 80-ms time window centered on the latency of the N1 response in the average waveform of each subject. Finally, single-trial latencies were calculated from the latencies of the corresponding amplitude peaks.

For each subject, single-trial N1 latencies and amplitudes obtained from the multiple linear regression method were averaged across trials and compared to the N1 latencies and amplitudes estimated manually from the averaged waveforms. Correlation coefficients and their significance were calculated and compared for N1 latency and amplitude separately.

#### Detection bias

In the described method, wavelet filtering is used to enhance the SNR of the N1 wave, and multiple linear regression is used to provide an accurate estimate of the latency and amplitude of the N1 wave at the level of single trials. To examine whether our method introduces any bias in the analysis, the same procedure was applied to the resting

EEG epochs obtained from all subjects. The obtained amplitude values were compared against zero using a one sample  $t$  test.

## Results

### Efficacy of different approaches for N1 detection in across-trial averages

Using the recommended montage (Kunde and Treede, 1993; Treede et al., 2003) (T3-Fz condition) the N1 wave was present in 5 out of 11 subjects (Fig. 3, left panel), with a latency of  $165 \pm 24$  ms and an amplitude of  $-2.6 \pm 3.4$   $\mu$ V (mean  $\pm$  SD). In the grand average waveform, its scalp distribution extended bilaterally towards temporal regions, with a clear maximum contralateral to the stimulated hand (Fig. 1, top left panel; Fig. 4).

In contrast, in the “C3-Fz” condition the N1 wave was present in all 11 subjects (Fig. 3, right panel), with a latency of  $167 \pm 25$  ms and a significantly larger amplitude of  $-4.3 \pm 2.8$   $\mu$ V ( $p < 0.001$ , two tailed paired  $t$  test). Similarly to the “T3-Fz” condition, in the grand average waveform its scalp distribution extended bilaterally towards temporal regions, with a clear maximum contralateral to the stimulated hand (Fig. 1, top right panel; Fig. 4).

The isolated number of ICs classified as “N2-related”, ranged, across subjects, from 1 to 2 ( $1.4 \pm 0.5$ ). These N2-related ICs accounted for  $25.5 \pm 12.8\%$  of the variance of the entire LEP response. The peak amplitudes of the N2 wave was significantly reduced ( $-55.2 \pm 20.6\%$ ;  $p < 0.0001$ , two-tailed paired  $t$  test) after the subtraction of N2-related ICs. For each subject, the number of N2-related ICs, the signal variance they explain and the N2-wave latency and amplitude before and after the removal of N2-related ICs are summarized in Table 1.

After the N2-related activity isolated with ICA was removed, in the “T3-Fz, N2-IC removed” condition the N1 wave was identified in 7 out of 11 subjects, with a latency of  $174 \pm 29$  ms and an amplitude of  $-3.3 \pm 3.1$   $\mu$ V. In the grand average waveform, its scalp distribution was restricted to the hemisphere contralateral to the stimulated hand, with a maximum at C3 (Fig. 1, bottom left panel; Figs. 4, 5).

In the “C3-Fz, N2-IC removed” condition the N1 wave was still present in all 11 subjects, with a latency of  $166 \pm 26$  ms and an amplitude of  $-4.2 \pm 2.4$   $\mu$ V. Similarly to the “T3-Fz, N2-IC removed” condition, in the grand average waveform its scalp distribution was restricted to the hemisphere contralateral to the stimulated hand, with a maximum at C3 (Fig. 1, bottom right panel; Fig. 4).

There was no significant main effect of the factors “montage” or “N2-IC removal” on the N1 latency ( $p = 0.577$  and  $p = 0.145$ , respectively), but there was an interaction between these two factors ( $p = 0.006$ ). Post hoc comparisons revealed that the N1 latency measured after the removal of the N2-related activity was significantly longer, but only when considering the Tc-Fz montage ( $p = 0.014$ , two tailed paired  $t$  test) (Fig. 4).

There was a significant main effect of the factor “montage” on the N1 amplitude ( $p = 0.024$ ), no main effect of the factor “N2-IC removal” ( $p = 0.682$ ), and a significant interaction between these two factors ( $p = 0.018$ ). Post hoc comparisons revealed that the N1 amplitude measured at T3-Fz was significantly smaller than the N1 amplitude measured at C3-Fz, but only when the N2-related activity was not removed ( $p < 0.001$ , two tailed paired  $t$  test) (Fig. 4).

### Single-trial analysis of N1 peak: wavelet filtering

In order to obtain a single-trial estimate of the N1 peak, the SNR of single-trial LEPs was increased by using a time–frequency filter based on the continuous wavelet transform (CWT). The left panel of Fig. 6 shows the time–frequency representation of the grand averaged N1 waveform used to derive the filter model. This representation is characterized by a phase-locked signal increase maximal between 100 and 350 ms (in time), and between 5 and 10 Hz (in frequency). This

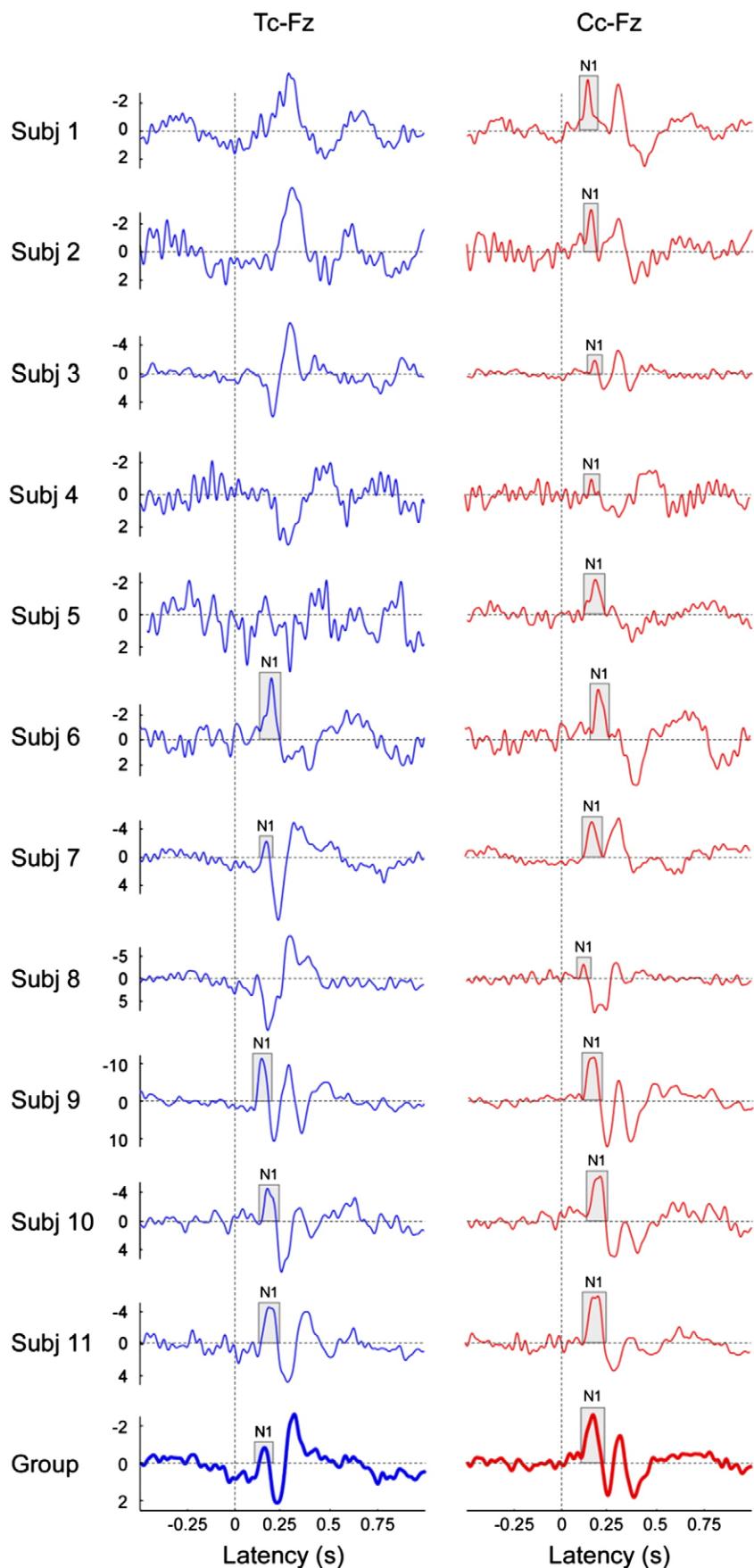


**Fig. 3.** Identification of N1 response in single subjects. Single-subject average ERP waveforms obtained using the Tc-Fz montage (left panel) and the Cc-Fz montage (right panel). Group averages are displayed in the bottom row. Note how, using the Tc-Fz montage, a clear N1 can be detect in 5 out of 11 subjects, while using the Cc-Fz montage a clear N1 can be detected in all subjects.

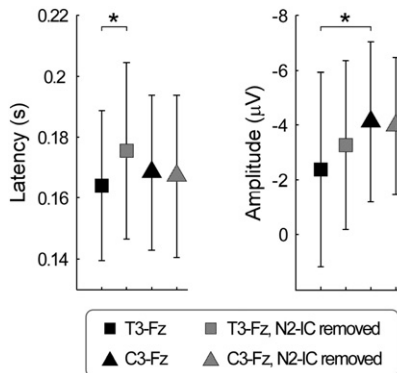


**Fig. 4.** Comparison of N1 latencies and amplitudes across the four explored conditions. Left panel: N1 latencies averaged across all subjects. Error bars represent variance across subjects, expressed as SD. Note how the N1 latency measured after the removal of the N2-related activity was significantly longer, but only when considering the Tc-Fz montage ( $p=0.014$ , two tailed paired  $t$  test). Right panel: N1 amplitudes averaged across all subjects. Error bars represent variance across subjects, expressed as SD. Note how the N1 amplitude measured at T3-Fz was significantly smaller than the N1 amplitude measured at C3-Fz, but only when the N2-related activity was not removed ( $p<0.001$ , two tailed paired  $t$  test).

representation, thresholded at 0.85, was used to generate the filter model that was subsequently applied to every single-trial LEP. The right panel of Fig. 6 shows how this CWT filter reduces minimally the amplitude of the response but increases remarkably its SNR (Table 2).

The bidimensional plots of single trial EEG responses in the left panel of Fig. 7 show the effect of the CWT filter on single-trial LEP waveforms and on single-trial resting EEG. While in the LEP waveforms the wavelet filtering significantly enhances the SNR of the phase-locked N1 wave (from  $6.7 \pm 3.4$  to  $16.4 \pm 9.5$ ,  $p=0.003$ , Wilcoxon test) (Table 2), in the resting EEG the wavelet filtering only reduces the noise. Single-subject SNRs of the N1 wave before and after wavelet filtering are displayed in Table 2. Single-subject N1 latencies before N2-removal, after N2-IC removal and after wavelet filtering are summarized in Table 3.

#### Comparison between standard-average and single-trial N1 values

Fig. 8 shows the correlations between the N1 latencies and amplitudes obtained from the multiple linear regression method and the N1 latencies and amplitudes estimated manually from the averaged waveforms.

The average of single-trial estimates of both N1 latency and N1 amplitude values showed a strong correlation with the corresponding values measured in standard averaged waveforms (N1 latency:  $R=0.9980$ ,  $p<0.0001$ ; N1 amplitude:  $R=0.9947$ ,  $p<0.0001$ ). The N1 latency values were almost identical (single trials:  $167 \pm 25$  ms;

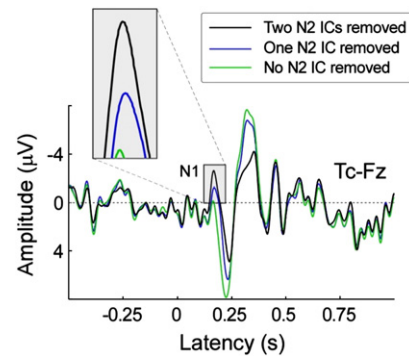


**Fig. 5.** Effect of the removal of the N2-related activities on the N1 waveform. Across-trial average waveforms from one representative subject. Waveforms are displayed using the Tc-Fz montage. The green line represents the original, unsubtracted signal. The blue line represents the waveform obtained after removal of one N2-related IC. The black line represents the waveform obtained after removal of all (two, in this case) N2-related ICs. Note how, by removing the N2-related ICs, the N1 peak becomes evident. An enlargement of the N1 peak is shown in the inset.

standard average:  $166 \pm 24$  ms;  $p=0.135$ , two tailed  $t$  test) (Fig. 8, left panel). In contrast, the N1 amplitude values were significantly greater in the single-trial estimates than in the standard averaged waveforms (single trials:  $-4.3 \pm 2.7$   $\mu$ V; standard average:  $-3.6 \pm 2.2$   $\mu$ V; +20% absolute increase,  $p<0.001$ , two tailed  $t$  test) (Fig. 8, right panel).

#### Detection bias

To test if the method used to estimate single-trial N1 amplitude introduced any detection bias, the same method was applied to an equal number of resting EEG epochs obtained from all subjects. The single-trial estimate of response amplitude from resting EEG epochs yielded a mean ( $\pm$ SD) amplitude value of  $0.05 \pm 5.1$   $\mu$ V. These amplitude values were not significantly different from zero ( $p=0.76$ , one sample  $t$  test). A comparison of the single-trial estimates obtained in the LEP waveforms vs. the resting EEG epochs in a representative subject is shown in the right panel of Fig. 7. This result confirms that the described method provides an unbiased estimate of single-trial N1 LEP amplitude.

#### Discussion

In this study we obtained four main findings. First, we suggest that the N1 wave of the LEP can be better detected using a central-frontal (C3-Fz) montage, compared to the recommended temporal-frontal (T3-Fz) montage. Second, we show that the N1 wave is optimally

**Table 1**

Number of and variance explained by N2-related ICs identified in each subject, as well as N2-wave latency and amplitude before and after the removal of N2-related ICs.

| Subject          | Number of N2-related ICs | Variance explained (%) | Before N2-IC removal |                         | After N2-IC removal |                         |
|------------------|--------------------------|------------------------|----------------------|-------------------------|---------------------|-------------------------|
|                  |                          |                        | N2 latency (ms)      | N2 amplitude ( $\mu$ V) | N2 latency (ms)     | N2 amplitude ( $\mu$ V) |
| #1               | 1                        | 10.8                   | 190                  | -38.3                   | 205                 | -22.3                   |
| #2               | 2                        | 22.2                   | 188                  | -17.3                   | 202                 | -3.3                    |
| #3               | 1                        | 17.4                   | 230                  | -28.3                   | 246                 | -16.1                   |
| #4               | 2                        | 21.2                   | 233                  | -18.2                   | 274                 | -5.3                    |
| #5               | 1                        | 19.1                   | 236                  | -13.2                   | 300                 | -5.3                    |
| #6               | 1                        | 40.0                   | 274                  | -9.1                    | 285                 | -1.9                    |
| #7               | 2                        | 49.2                   | 236                  | -13.9                   | 203                 | -5.3                    |
| #8               | 1                        | 24.9                   | 224                  | -19.9                   | 209                 | -14.8                   |
| #9               | 2                        | 43.5                   | 179                  | -10.4                   | 176                 | -8.3                    |
| #10              | 1                        | 9.2                    | 224                  | -8.3                    | 186                 | -4.0                    |
| #11              | 1                        | 25.8                   | 198                  | -14.6                   | 215                 | -4.1                    |
| Mean ( $\pm$ SD) | $1.4 \pm 0.5$            | $25.5 \pm 12.8$        | $219 \pm 28$         | $-17.4 \pm 9.0$         | $227 \pm 42$        | $-8.2 \pm 6.5$          |

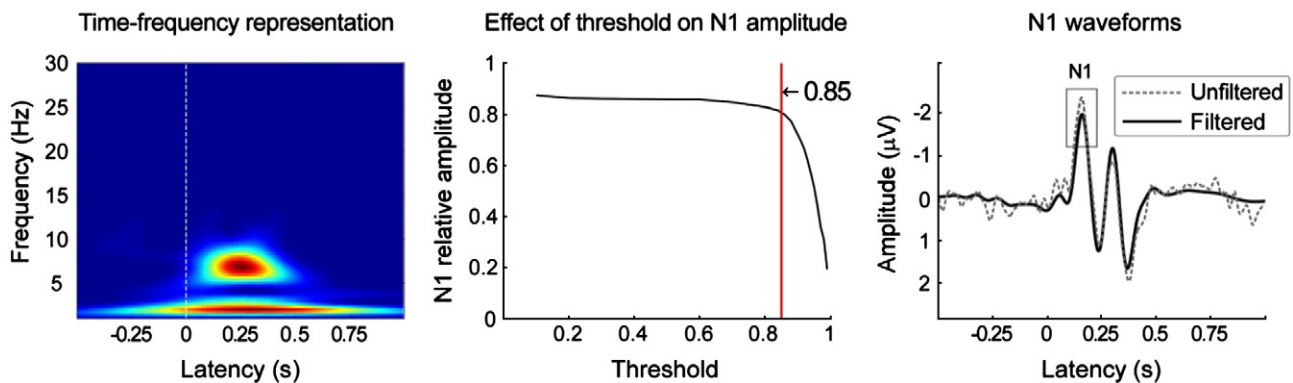


**Fig. 6.** Wavelet filtering and its effect on the N1 response. Left panel: time-frequency representation of the average laser-evoked response at C3-Fz after the removal of the N2-related ICs ("C3-Fz, N2-IC removed" condition). x-axis: latency (s); y-axis: frequency (Hz). For each frequency, the magnitude of power spectrum was normalized by subtracting the average amplitude from the foreperiod between  $-0.25$  and  $0$  s. Middle panel: threshold estimation and wavelet filtering effect. x-axis: threshold; y-axis: ratio between filtered and unfiltered N1 peak amplitude. The reduction of the N1 peak amplitude is expressed as a function of the applied threshold. Note how the amplitude of the filtered N1 peak is reduced by applying a higher threshold. A threshold of  $0.85$  (red line) was chosen as the best compromise between preserving the N1 response and increasing its SNR. Right panel: effect of the wavelet filtering on the N1 waveforms. x-axis: latency (s); y-axis: amplitude ( $\mu$ V). Note how the SNR of the filtered N1 waveform (solid line) is significantly increased compared to the original unfiltered waveform (dashed line) (from  $6.7 \pm 3.4$  to  $16.4 \pm 9.5$ ,  $p = 0.003$ , Wilcoxon test; see also Table 2).

detected when the neural activities underlying the N2 wave, which interfere with the scalp expression of the N1 wave, are isolated and removed in a preliminary step using ICA. Third, we show that after the N2-related activities are removed, the SNR of the N1 LEP response can be effectively enhanced using a novel approach based on wavelet filtering. Fourth, we provide quantitative evidence that a multiple linear regression approach can be applied to these LEP waveforms with higher SNR to obtain an automatic, reliable and unbiased estimate of the peak latency and amplitude of the N1 wave, both in average and single-trial waveforms.

#### N1 recording montage

The scalp distribution of LEPs around the peak latency of the N1 wave displays a maximal positivity in the frontal midline region (Kunde and Treede, 1993; Treede et al., 2003). Therefore, Fz has been suggested as being the best choice for a reference electrode to detect the N1 negative peak in a bipolar montage, and a waveform displayed using the contralateral temporal electrode Tc versus Fz is currently recommended to detect the N1 response (Crucu et al., 2008; Treede et al., 2003). On the other hand, there is evidence that the amplitude of the N1 is similar in the Tc-Fz and in the Cc-Fz montages. For instance, Legrain et al. (2002) found similar N1 amplitudes at temporal (T3/T4) and central (C3/C4) electrodes, and even higher N1 amplitudes at C4 when considering left hand stimulation (see upper panel of Fig. 8 in their publication). Also, the topography of the N1 wave (see Fig. 1 of their publication) shows a clear N1 maximum at central, and not temporal electrodes. In a very recent study, Legrain

et al. (2009) observed that "N1c was not different between right temporo-parietal (T4 and TP8) and centro-parietal (C4 and CP4) electrodes." So far, exploring experimental modulations of the N1 wave has been limited because of the difficulty to identify a clear N1 response in single subjects or patients when using this recommended montage. For example, in the present study, a clear N1 response was identified in only 5 out of 11 subjects (Fig. 3, left panel). Several reasons could explain the difficulty to detect a clear N1 wave using the Tc-Fz montage. First, when this montage is used, the scalp expression of the N1 wave is suppressed by the overlapping N2 wave, which has an opposite polarity. Second, the Tc electrode is particularly sensitive to artifacts related to the activity of the *temporalis* muscle. Both of these factors contribute to reduce the SNR of the N1 wave when the Tc-Fz montage is used. Importantly, the scalp distribution of LEPs at or around the peak latency of the N1 wave displays a maximal negativity either between the contralateral temporal (Tc) and central (Cc) electrodes (e.g. Tarkka and Treede, 1993) or centred over the central (Cc) electrode (Fig. 1, top panel). For this reason, and because electrode Cc is less affected by activity of the *temporalis* muscle, we compared the N1 response in the recommended Tc-Fz montage with the N1 response in the Cc-Fz montage. By performing this comparison, we found that in the Cc-Fz montage, there is much less interference between the scalp expressions of the N2 and N1 waves. Indeed, when the N2-related activity was isolated using ICA (Fig. 1, middle panel; see also Fig. 9 in Mouraux and Iannetti, 2008), its amplitude was similar at Cc and Fz electrodes. Thus, its scalp expression is largely cancelled out using the Cc-Fz bipolar montage.

Consequently, in the Cc-Fz montage we were able to detect a clear N1 response in all 11 subjects, as opposed to only 5 out of 11 subjects when using the Tc-Fz montage (Fig. 1; Fig. 3). Furthermore, its peak amplitude was significantly larger in the Cc-Fz montage than in the Tc-Fz montage (Fig. 1, top panel; Fig. 4).

**Table 2**  
SNR of the N1 wave before and after wavelet filtering.

| Subject          | Before wavelet filtering | After wavelet filtering |
|------------------|--------------------------|-------------------------|
| #1               | 12.4                     | 38.1                    |
| #2               | 4.3                      | 15.2                    |
| #3               | 6.4                      | 10.3                    |
| #4               | 6.5                      | 17                      |
| #5               | 2.3                      | 9.4                     |
| #6               | 10                       | 24.2                    |
| #7               | 11.3                     | 26.1                    |
| #8               | 2.8                      | 13.9                    |
| #9               | 7.2                      | 8.3                     |
| #10              | 4.1                      | 7.4                     |
| #11              | 6.2                      | 11                      |
| Mean ( $\pm$ SD) | $6.7 \pm 3.4$            | $16.4 \pm 9.5$          |

#### Spatial-temporal filtering to remove the interference between N1 and N2 waves

The overlap in time and space between the N1 and N2 waves (Kunde and Treede, 1993; Treede et al., 1988) may influence the N1 amplitude greatly, and, when using the Tc-Fz montage, may even lead to a positive absolute amplitude value for the N1 negative deflection relative to baseline (Fig. 5). In order to reduce the interference due to the overlap between the N1 and the N2 waves, we used ICA to isolate and remove N2-related neural activities contributing to the EEG signal (Fig. 1, middle and bottom panels). ICA is a blind source separation technique that works as a spatial filter and is capable to exploit the

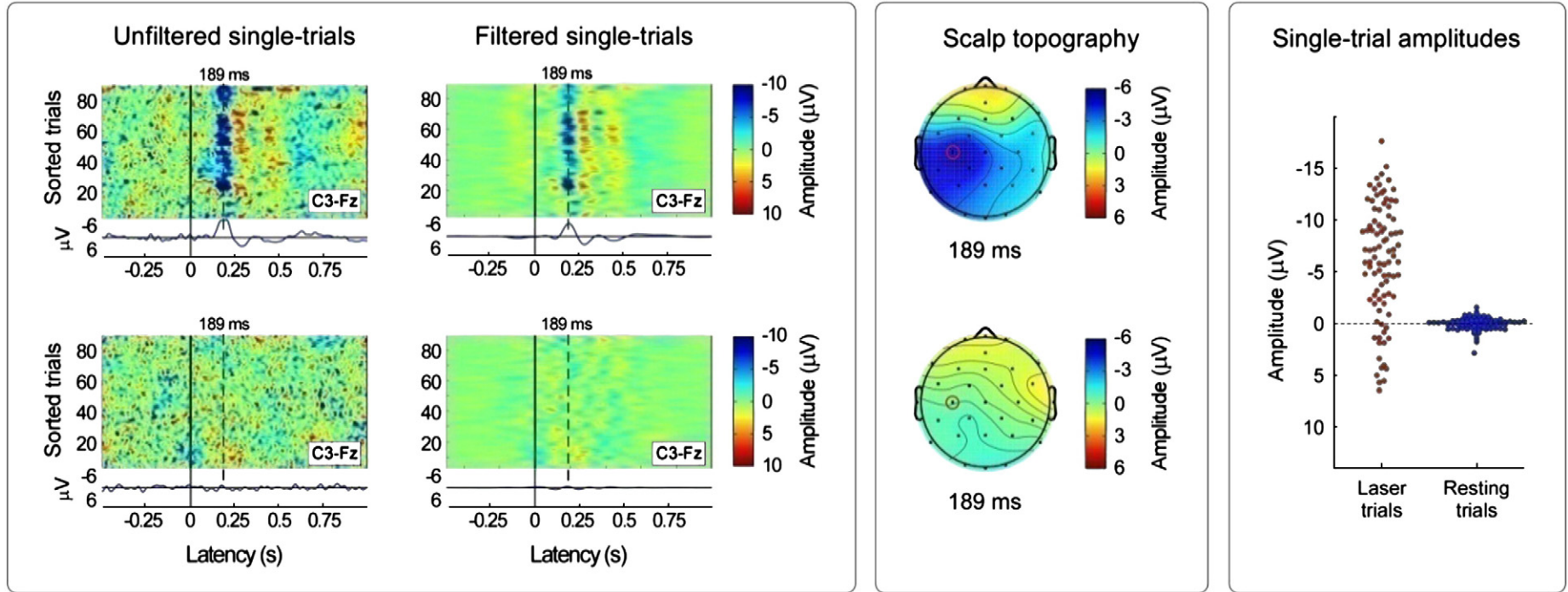


**Fig. 7.** Unbiased automatic detection of single-trial N1 amplitudes. Left panel: comparison of the effect of wavelet filtering on stimulus-evoked EEG trials (obtained from the “C3-Fz, N2-IC removed” condition, top row) and resting EEG trials (obtained from the same montage, bottom row). Ninety single-trials from one subject are represented using bidimensional plots. Horizontal lines in the plot represent single-trial responses, with signal amplitude colour-coded at each time point. Responses are sorted vertically in order of occurrence, from bottom (first trial) to top (last trial). The waveform below each plot is the average of all responses. Negativity is plotted upward. The dashed line marks the latency of the N1 peak in the filtered waveform. Middle panel: scalp topography of the average of stimulus-evoked EEG trials (top) and resting EEG trials (bottom), at the peak latency of the N1 wave in the filtered waveform. Note how the topography of stimulus-evoked trials is characterized by a contralateral negative peak, maximum around the C3 electrode (red circle). Right panel: single-trial amplitudes (same data shown in the left and middle panel) estimated in stimulus-evoked EEG trials (in red) and resting EEG trials (in blue), using multiple linear regression. The average N1 peak amplitude is  $-6.0 \pm 5.6 \mu\text{V}$  in the stimulus-evoked trials and  $-0.05 \pm 0.6 \mu\text{V}$  in the resting EEG trials. Note how the amplitude values obtained from the resting EEG trials are not significantly different from zero ( $p = 0.4239$ , one sample  $t$  test).

**Table 3**

Effect of N2-IC removal and wavelet filtering on the N1 latency (ms).

| Subject          | Before N2-IC removal | After N2-IC removal | After wavelet Filtering |
|------------------|----------------------|---------------------|-------------------------|
| #1               | 154                  | 140                 | 142                     |
| #2               | 125                  | 123                 | 130                     |
| #3               | 167                  | 166                 | 166                     |
| #4               | 199                  | 194                 | 201                     |
| #5               | 166                  | 166                 | 173                     |
| #6               | 200                  | 199                 | 194                     |
| #7               | 201                  | 200                 | 196                     |
| #8               | 168                  | 168                 | 162                     |
| #9               | 136                  | 136                 | 140                     |
| #10              | 153                  | 155                 | 157                     |
| #11              | 172                  | 174                 | 170                     |
| Mean ( $\pm$ SD) | 167 $\pm$ 25         | 166 $\pm$ 26        | 166 $\pm$ 24            |

spatial information contained in multichannel EEG recordings to separate sensory ERPs into distinct ICs, each having a fixed scalp distribution and a maximally-independent time course (Makeig et al., 1997, 2004; Mouraux and Iannetti, 2008). ICA has been demonstrated to be effective in isolating stimulus-related and ongoing components in single-trial EEG signals (Debener et al., 2006; Jung et al., 2001; Tang et al., 2005), and has been also applied to the separation of LEPs into physiologically-distinct neural components (Mouraux and Iannetti, 2008, 2009).

After the removal of N2-related activities, the grand-average waveform obtained using the recommended Tc-Fz montage was remarkably different (Fig. 1, bottom left panel; Fig. 5). The peak amplitude of the N1 wave was significantly increased (by ~26%), while the subsequent N2 wave, which appears as a positive deflection in this montage, virtually disappeared. In addition, removing N2-related activities significantly increased the average peak latency of the N1 wave (from  $165 \pm 26$  ms to  $174 \pm 30$  ms,  $p = 0.014$ , two tailed paired  $t$  test) (Fig. 4), thus showing how the N2-related activities exert a stronger interfering effect at latencies closer to the peak of the N2 wave. Importantly, removing N2-related activities did not significantly modify the N1 wave displayed using the Cc-Fz montage (see Fig. 1, bottom right panel), and both the latency and the amplitude of the N1 peak were almost identical before and after the removal of N2-related activities (Fig. 4). This observation is due to the fact that in the Cc-Fz montage the N2-related activities are already largely cancelled out. After the removal of N2-related activities, the

scalp distribution of LEPs around the peak latency of the N1 wave were markedly more lateralized, displaying a negative maximum between Tc and Cc electrodes, slightly greater at Cc (bottom panel of Fig. 1). This scalp expression is compatible with the hypothesized location of its cortical generators (Garcia-Larrea et al., 2003), i.e. the operculo-insular region and, possibly, the primary somatosensory cortex contralateral to the stimulated side. Furthermore, this location confirms that to obtain a reliable estimate of the N1 wave, the Cc-Fz montage is better suited than the Tc-Fz montage.

In previous studies, ICA has been applied successfully to separate large-amplitude components of the LEP response (Mouraux and Iannetti, 2008, 2009), but its application to isolate small-amplitude components like the N1 wave has never been described so far. In the present study, ICA was not able to isolate N1-related activities consistently in all subjects, probably because of their low SNR. For this reason we chose to enhance the SNR of the N1 wave indirectly, by removing N2-related activities that interfere with the scalp expression of the N1 neural components.

#### Time-frequency filtering to enhance the SNR of the N1 wave

Several methods have been proposed to enhance the SNR of single-trial ERP responses to sensory stimuli, both in the time domain (Doyle, 1975; Nishida et al., 1993; Rossi et al., 2007) and in the time-frequency domain (Jongsma et al., 2006; Mouraux and Plaghki, 2004; Quiroga and Garcia, 2003; Quiroga, 2000; Wang et al., 2007). Nishida et al. (1993) used a method based on the combination of three band-pass filters and Rossi et al. (2007) applied an autoregressive filter with exogenous input to enhance the SNR of single-trial somatosensory ERP waveforms. Some studies (Quiroga, 2000; Quiroga and Garcia, 2003; Jongsma et al., 2006) adopted a discrete wavelet transform (DWT) to retain only wavelet coefficients correlating with the ERP signal, and thereby generate a denoised average ERP waveform. Using a method similar to the one developed in Mouraux and Plaghki (2004), we applied a time-frequency filter based on the continuous wavelet transform to the ICA-filtered EEG data (summarized in Fig. 2, top panel). The filter was generated by thresholding the group average time-frequency representation of the LEP in order to achieve the highest SNR. Indeed, as the N1 wave is smaller than the N2 and P2 waves, the N1 wave also has smaller weight on the time-frequency plane. Thus, in some subjects, the N1 wave may not be clearly represented in the time-

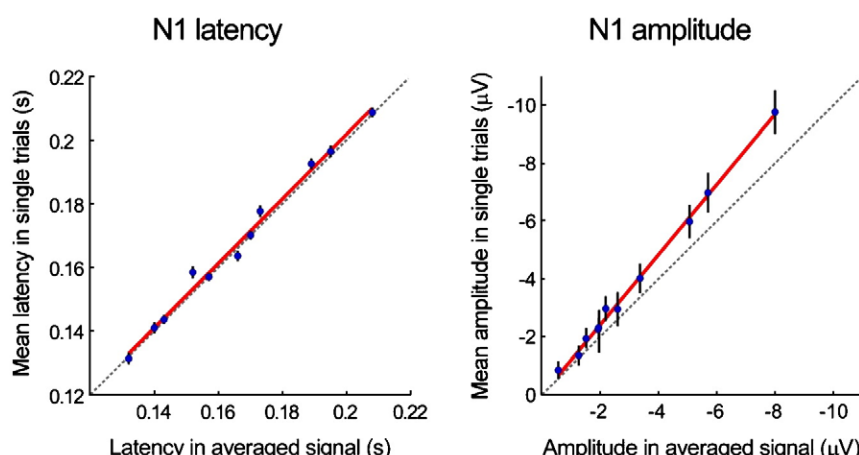


**Fig. 8.** Correlations between the average N1 latencies and amplitudes obtained from the multiple linear regression method and the N1 latencies and amplitudes estimated manually from the averaged waveforms. Significant correlations were observed when examining both N1 latencies ( $R = 0.9980$ ,  $p < 0.0001$ ; left panel) and N1 amplitudes ( $R = 0.9947$ ,  $p < 0.0001$ ; right panel). Each point represents the values from one subject. Vertical error bars represent, for each subject, the variance across trials (expressed as SEM). Black dashed lines represent the identity lines, and red solid lines represent the best linear fit. Note how the N1 latency values obtained from the two measurements are almost identical ( $p = 0.135$ , two-tailed  $t$  test), while the N1 amplitude values were significantly greater in the single-trial estimates than in the standard averaged waveforms (with an average + 20% increase;  $p < 0.001$ , two-tailed  $t$  test).

frequency domain. For these reasons, we believe that generating the wavelet filter using the group average waveform would yield more robust results. Compared to filtering in the time domain, filtering in the time–frequency domain filters the signal both as a function of time and frequency (i.e. frequency bands are weighted differently as a function of time). Thus, this approach is optimal to explore the time varying frequency spectra of event-related brain responses.

Accordingly, we show that such a wavelet filtering procedure (Fig. 2, top panel) can be successfully applied to enhance the SNR of the N1 wave of LEPs (Fig. 7). It is important to highlight that this procedure does not generate spurious N1 waves when applied to the resting EEG signal (Fig. 7). This lack of detection bias is due to the fact that, in each single EEG epoch, the wavelet filter maximizes the signal corresponding to the time–frequency representation of the event-related response regardless of its phase (i.e. regardless of its positive or negative polarity).

DWT-based denoising approaches have been widely used in biomedical signal processing (Quiroga, 2000; Quiroga and Garcia, 2003; Jongasma et al., 2006). However, DWT only operates at specific scales and transitions (generally, at dyadic scales and transitions). In contrast, CWT (Mouraux and Iannetti, 2008; Tognola et al., 1998) can be performed at every possible scale/frequency and transition (generally, at uniform frequency grids and every possible time points). Thus, CWT can analyze the ERP signal in a more refined scale, at the expense of high computational complexity.

#### *N1 peak in single-trial LEPs: automatic measurement*

We have recently described a method using a multiple linear regression approach to obtain single-trial estimates of the latency and amplitude of event-related potentials, and showed that this method effectively estimates the peak latency and amplitude of the N2 and P2 waves of LEPs (Mayhew et al., 2006).

Here, we show that after removing the N2-related neural activities from the single trial LEP waveforms using a spatio-temporal filter based on ICA (Fig. 1), and after enhancing the SNR of the N1 wave using a time–frequency filter based on the continuous wavelet transform (Fig. 6), a multiple linear regression approach similar to the one we already developed (Mayhew et al., 2006) can be used to obtain a fast and unbiased estimate of the peak latency and amplitude of the N1 wave at the level of single trials. This procedure is summarized in the bottom panel of Fig. 2. Briefly, for each subject, a regressor and its temporal derivative are obtained from the across-trial average waveform. This basis set is then regressed against each single EEG epoch, thus providing a quantitative measure of peak latency and amplitude of the N1 wave present in each single LEP epoch. Including the temporal derivative, a procedure commonly used to analyze functional MRI data (Friston et al., 1998) presents the advantage of modeling the temporal variability of the responses and provides an estimate of single-trial peak latency of the N1 wave. Importantly, this method allows modeling the amplitude of each single trial regardless of its phase (i.e. regardless of its positive or negative polarity). Therefore, if a sufficient number of trials are considered, the contribution of non-event-related peaks in the signal will cancel out and tend towards zero. For this reason, when we applied the multiple linear regression to the resting EEG data, the average amplitude of the single-trial estimates of the N1 peak was negligible ( $0.05 \mu\text{V}$ ; not significantly different from zero,  $p = 0.76$ ) (Fig. 7, right panel).

Across subjects, the average of single-trial estimates of N1 latency and amplitude correlated remarkably well with the corresponding values measured using the waveforms averaged across trials (Fig. 8). While the average of estimated single-trial N1 latencies was almost identical to those measured in the averaged waveforms, the average of estimated single-trial N1 amplitudes was significantly larger in the single-trial estimate than in the average waveforms (Fig. 8). This

difference is likely to be due to the across-trial latency jitter, which results in averaging N1 waves with slightly different phases, thus distorting its shape and reducing its amplitude in the average waveform. Importantly, the increase in peak amplitude obtained by measuring the response in single trials was much smaller for the N1 wave (+20%) than for the N2 and P2 waves (approximately +65% and +30%, respectively) (Mayhew et al., 2006). This finding indicates that the latency jitter of the N1 wave is significantly smaller than the latency jitter of the N2 and P2 waves of LEPs. Considering that the N1 wave is more transient than the N2 and P2 waves (i.e. the N1 has higher frequency content than the N2 and P2), across-trial averaging would distort it more than N2 and P2 waves. Hence, if the latency jitter affecting the N1, N2 and P2 waves was similar, the gain in amplitude resulting from measuring the N1 wave in single trials should be greater than the gain in amplitude resulting from measuring the N2 and P2 waves in single trials. Therefore, the fact that the opposite was observed indicates that the N1 wave is affected by less latency jitter than the later N2 and P2 waves. Accordingly, the across-trial variability (expressed as SD) of the peak latency of the N1 wave (which is a direct measure of response jitter) is 17.8 ms, while that for the N2 and P2 waves are 63.5 and 87.2 ms, respectively (Mayhew et al., 2006). This is consistent with the notion that earlier-latency, more exogenous responses (like the N1 wave, Lee et al., 2009) have a smaller latency jitter than longer latency, more endogenous responses (like the N2 and P2 waves of the LEPs, Mouraux and Iannetti, 2009).

#### *Advantages of the proposed method*

The problem of how to treat ERP waveforms in which expected peaks cannot be identified visually is important, and has yet to be satisfactorily addressed. This issue is especially relevant in studies examining an experimental modulation of ERPs leading to a strong response attenuation, or in conditions in which their SNR is particularly low (e.g. in patient studies or in simultaneous recording of EEG during fMRI, Iannetti et al., 2005a). Average waveforms without an apparent ERP response are usually either discarded from subsequent analyses, or arbitrarily assigned a response magnitude corresponding to zero. Discarding these average waveforms, besides constituting a loss of physiologically-relevant information, biases the results towards an underestimate of the effect of the experimental modulation or of the deficit caused by the underlying disease. Conversely, arbitrarily assigning zero amplitude values to these undetectable responses will inevitably introduce a bias in the opposite direction, i.e. it will overestimate the effect of the experimental modulation or of the deficit caused by the underlying disease.

The automated method of estimating ERP latency and amplitude described in the present study successfully addresses this problem, because it always assigns a latency and amplitude value to each single trial or average waveform. Importantly, when the stimulus does not elicit any ERP response, the across-trial average of the single-trial estimates of amplitude will tend towards zero. Nevertheless, even in the presence of a barely-detectable response, the across-trial average of the single-trial estimates of amplitude will be different from zero, thus providing a reliable estimate of the amount of stimulus-evoked response in the recorded trials.

Another advantage of the method described in the present study is that the obtained estimate is entirely independent of the subjective interpretation of the researcher. Consequently, whereas the results from a manual analysis of N1 amplitude would vary if performed by different researcher or by the same researcher in different days, the estimates obtained with an automated analysis are reproducible and comparable across experiments and laboratories.

Finally, we show that our approach allows obtaining an accurate estimate of the latency and amplitude of the N1 wave of LEPs, both in

average waveforms and single trials. We believe that the automated approach to single-trial measurement of the N1 wave of LEPs opens new possibilities to explore the nociceptive system both in basic and clinical research, considering that the use of N1 has been recommended to enhance the clinical sensitivity of LEPs (Crucu et al., 2008), and that its physiological role has been recently partly clarified (e.g. Iannetti et al., 2008; Lee et al., 2009; Legrain et al., 2002; Mouraux and Iannetti, 2009).

## Acknowledgments

The authors are grateful to Dr ZG Zhang and members of the GAMFI Centre for their insightful comments. LH is supported by the Lee Wing Tat Medical Research Fund. AM is supported by the Belgian National Fund for Scientific Research (FNRS). GDI is University Research Fellow of The Royal Society, and acknowledges the support of the BBSRC.

## References

- Baumgartner, U., Crucu, G., Iannetti, G.D., Treede, R.D., 2005. Laser guns and hot plates. *Pain* 116, 1–3.
- Bromm, B., Treede, R.D., 1984. Nerve fibre discharges, cerebral potentials and sensations induced by CO<sub>2</sub> laser stimulation. *Hum. Neurobiol.* 3, 33–40.
- Carmon, A., Mor, J., Goldberg, J., 1976. Evoked cerebral responses to noxious thermal stimuli in humans. *Exp. Brain Res.* 25, 103–107.
- Carmon, A., Friedman, Y., Coger, R., Kenton, B., 1980. Single trial analysis of evoked potentials to noxious thermal stimulation in man. *Pain* 8, 21–32.
- Crucu, G., Aminoff, M.J., Curio, G., Guerit, J.M., Kakigi, R., Mauguire, F., Rossini, P.M., Treede, R.D., Garcia-Larrea, L., 2008. Recommendations for the clinical use of somatosensory-evoked potentials. *Clin. Neurophysiol.* 119, 1705–1719.
- Dawson, G.D., 1951. A summation technique for detecting small signals in a large irregular background. *J. Physiol.* 115, 2p–3p.
- Dawson, G.D., 1954. A summation technique for the detection of small evoked potentials. *Electroencephalogr. Clin. Neurophysiol.* 6, 65–84.
- Debener, S., Ullsperger, M., Siegel, M., Engel, A.K., 2006. Single-trial EEG-fMRI reveals the dynamics of cognitive function. *Trends Cogn. Sci.* 10, 558–563.
- Debener, S., Strobel, A., Sorger, B., Peters, J., Kranczoch, C., Engel, A.K., Goebel, R., 2007. Improved quality of auditory event-related potentials recorded simultaneously with 3-T fMRI: removal of the ballistocardiogram artefact. *NeuroImage* 34, 587–597.
- Delorme, A., Makeig, S., 2004. EEGLAB: an open source toolbox for analysis of single-trial EEG dynamics including independent component analysis. *J. Neurosci. Methods* 134, 9–21.
- Doyle, D.J., 1975. Some comments on the use of Wiener filtering for the estimation of evoked potentials. *Electroencephalogr. Clin. Neurophysiol.* 38, 533–534.
- Ellrich, J., Jung, K., Ristic, D., Yekta, S.S., 2007. Laser-evoked cortical potentials in cluster headache. *Cephalgia* 27, 510–518.
- Friston, K.J., Fletcher, P., Josephs, O., Holmes, A., Rugg, M.D., Turner, R., 1998. Event-related fMRI: characterizing differential responses. *NeuroImage* 7, 30–40.
- Garcia-Larrea, L., Frot, M., Valeriani, M., 2003. Brain generators of laser-evoked potentials: from dipoles to functional significance. *Neurophysiol. Clin.* 33, 279–292.
- Haig, A.R., Gordon, E., Rogers, G., Anderson, J., 1995. Classification of single-trial ERP sub-types: application of globally optimal vector quantization using simulated annealing. *Electroencephalogr. Clin. Neurophysiol.* 94, 288–297.
- Iannetti, G.D., Truini, A., Romaniello, A., Galeotti, F., Rizzo, C., Manfredi, M., Crucu, G., 2003. Evidence of a specific spinal pathway for the sense of warmth in humans. *J. Neurophysiol.* 89, 562–570.
- Iannetti, G.D., Niazy, R.K., Wise, R.G., Jezzard, P., Brooks, J.C., Zambreanu, L., Vennart, W., Matthews, P.M., Tracey, I., 2005a. Simultaneous recording of laser-evoked brain potentials and continuous, high-field functional magnetic resonance imaging in humans. *NeuroImage* 28, 708–719.
- Iannetti, G.D., Zambreanu, L., Crucu, G., Tracey, I., 2005b. Operculoinsular cortex encodes pain intensity at the earliest stages of cortical processing as indicated by amplitude of laser-evoked potentials in humans. *Neuroscience* 131, 199–208.
- Iannetti, G.D., Zambreanu, L., Tracey, I., 2006. Similar nociceptive afferents mediate psychophysical and electrophysiological responses to heat stimulation of glabrous and hairy skin in humans. *J. Physiol.* 577, 235–248.
- Iannetti, G.D., Hughes, N.P., Lee, M.C., Mouraux, A., 2008. Determinants of laser-evoked EEG responses: pain perception or stimulus saliency? *J. Neurophysiol.* 100, 815–828.
- Jongsma, M.L.A., Eichele, T., Van Rijn, C.M., Coenen, A.M.L., Hugdahl, K., Nordby, H., Quiroga, R.Q., 2006. Tracking pattern learning with single-trial event-related potentials. *Clin. Neurophysiol.* 117, 1957–1973.
- Jung, T.P., Makeig, S., Westerfield, M., Townsend, J., Courchesne, E., Sejnowski, T.J., 2001. Analysis and visualization of single-trial event-related potentials. *Hum. Brain Mapp.* 14, 166–185.
- Kunde, V., Treede, R.D., 1993. Topography of middle-latency somatosensory evoked potentials following painful laser stimuli and non-painful electrical stimuli. *Electroencephalogr. Clin. Neurophysiol.* 88, 280–289.
- Lawless, J.F., 2003. Statistical models and methods for lifetime data, 2nd ed. Wiley, Hoboken, NJ.
- Lee, M.C., Mouraux, A., Iannetti, G.D., 2009. Characterizing the cortical activity through which pain emerges from nociception. *J. Neurosci.* 29, 7909–7916.
- Legrain, V., Guerit, J.M., Bruyer, R., Plaghki, L., 2002. Attentional modulation of the nociceptive processing into the human brain: selective spatial attention, probability of stimulus occurrence, and target detection effects on laser evoked potentials. *Pain* 99, 21–39.
- Legrain, V., Perchet, C., Garcia-Larrea, L., 2009. Involuntary orienting of attention to nociceptive events: neural and behavioral signatures. *J. Neurophysiol.* 102, 2423–2434.
- Makeig, S., Jung, T.P., Bell, A.J., Ghahremani, D., Sejnowski, T.J., 1997. Blind separation of auditory event-related brain responses into independent components. *Proc. Natl. Acad. Sci. U. S. A.* 94, 10979–10984.
- Makeig, S., Debener, S., Onton, J., Delorme, A., 2004. Mining event-related brain dynamics. *Trends Cogn. Sci.* 8, 204–210.
- Mayhew, S.D., Iannetti, G.D., Woolrich, M.W., Wise, R.G., 2006. Automated single-trial measurement of amplitude and latency of laser-evoked potentials (LEPs) using multiple linear regression. *Clin. Neurophysiol.* 117, 1331–1344.
- Mayhew, S.D., Dirckx, S.G., Niazy, R.K., Iannetti, G.D., Wise, R.G., 2010. EEG signatures of auditory activity correlate with simultaneously recorded fMRI responses in humans. *NeuroImage* 49, 849–864.
- Mouraux, A., Iannetti, G.D., 2008. Across-trial averaging of event-related EEG responses and beyond. *Magn. Reson. Imaging* 26, 1041–1054.
- Mouraux, A., Iannetti, G.D., 2009. Nociceptive laser-evoked brain potentials do not reflect nociceptive-specific neural activity. *J. Neurophysiol.* 101, 3258–3269.
- Mouraux, A., Plaghki, L., 2004. Single-trial detection of human brain responses evoked by laser activation of Adelta-nociceptors using the wavelet transform of EEG epochs. *Neurosci. Lett.* 361, 241–244.
- Mouraux, A., Guerit, J.M., Plaghki, L., 2003. Non-phase locked electroencephalogram (EEG) responses to CO<sub>2</sub> laser skin stimulations may reflect central interactions between A partial differential- and C-fibre afferent volleys. *Clin. Neurophysiol.* 114, 710–722.
- Nishida, S., Nakamura, M., Shibasaki, H., 1993. Method for single-trial recording of somatosensory evoked potentials. *J. Biomed. Eng.* 15, 257–262.
- Pfurtscheller, G., Lopes da Silva, F.H., 1999. Event-related EEG/MEG synchronization and desynchronization: basic principles. *Clin. Neurophysiol.* 110, 1842–1857.
- Quian Quiroga, R., Garcia, H., 2003. Single-trial event-related potentials with wavelet denoising. *Clin. Neurophysiol.* 114, 376–390.
- Quian Quiroga, R., 2000. Obtaining single stimulus evoked potentials with wavelet denoising. *Phys. D-Nonlinear Phenom.* 145, 278–292.
- Rossi, L., Bianchi, A.M., Merzagora, A., Gaggiani, A., Cerutti, S., Bracchi, F., 2007. Single trial somatosensory evoked potential extraction with ARX filtering for a combined spinal cord intraoperative neuromonitoring technique. *Biomed. Eng. Online* 6, 2.
- Schmahl, C., Greffrath, W., Baumgartner, U., Schlereth, T., Magerl, W., Philipsen, A., Lieb, K., Bohus, M., Treede, R.D., 2004. Differential nociceptive deficits in patients with borderline personality disorder and self-injurious behavior: laser-evoked potentials, spatial discrimination of noxious stimuli, and pain ratings. *Pain* 110, 470–479.
- Spencer, K.M., 2005. Averaging, detection, and classification of single-trial ERPs. In: Handy, T.C. (Ed.), *Event-related potentials : a methods handbook*. MIT Press, Cambridge, Mass., pp. 209–227.
- Tang, A.C., Sutherland, M.T., McKinney, C.J., 2005. Validation of SOBI components from high-density EEG. *NeuroImage* 25, 539–553.
- Tarkka, I.M., Treede, R.D., 1993. Equivalent electrical source analysis of pain-related somatosensory evoked potentials elicited by a CO<sub>2</sub> laser. *J. Clin. Neurophysiol.* 10, 513–519.
- Tognola, G., Grandori, F., Ravazzani, P., 1998. Wavelet analysis of click-evoked otoacoustic emissions. *IEEE Trans. Biomed. Eng.* 45, 686–697.
- Treede, R.D., Kief, S., Holzer, T., Bromm, B., 1988. Late somatosensory evoked cerebral potentials in response to cutaneous heat stimuli. *Electroencephalogr. Clin. Neurophysiol.* 70, 429–441.
- Treede, R.D., Lorenz, J., Baumgartner, U., 2003. Clinical usefulness of laser-evoked potentials. *Neurophysiol. Clin.* 33, 303–314.
- Treede, R.D., Meyer, R.A., Campbell, J.N., 1998. Myelinated mechanically insensitive afferents from monkey hairy skin: heat-response properties. *J. Neurophysiol.* 80, 1082–1093.
- Wang, Z., Maier, A., Leopold, D.A., Logothetis, N.K., Liang, H., 2007. Single-trial evoked potential estimation using wavelets. *Comput. Biol. Med.* 37, 463–473.